J Ind Microbiol Biotechnol (2012) 39:1061–1071
DOI 10.1007/s10295-012-1107-z

Analyzing the dynamics of cell growth and protein production in mammalian cell fed-batch systems using logistic equations

Chetan T. Goudar

Received: 1 January 2012 / Accepted: 9 February 2012 / Published online: 3 March 2012

Abstract The logistic modeling approach was used to describe experimental viable cell density (X) and product concentration (P) data from two industrial fed-batch mammalian cell culture processes with maximum product concentrations in the 3.0–9.4 g/l range. In both cases, experimental data were well described by the logistic equations and the resulting specific growth rate and protein productivity profiles provided useful insights into the process kinetics. Subsequently, sensitivity equations for both the X and P models were analyzed which helped characterize the influence of model parameters on X and P time courses. This was augmented by conventional sensitivity analyses where five values of each model parameter, 25% apart, were used to generate X and P time courses. Finally, results from sensitivity analysis were used to simulate X and P time courses that were reflective of typical early- and late-stage fed-batch cell culture processes. Different combinations of the logistic model parameters were used to arrive at the same final product concentration demonstrating the ability of the logistic approach to describe the multitude of process paths that result in the same final product concentration. Overall, the capability of the logistic equations to well describe X and P data from fed-batch cultures, coupled with their ability to simulate the multitude of paths leading up to the desired cell density and product concentration profiles, make them a useful tool during mammalian cell fed-batch process development.

C. T. Goudar (✉)
Cell Culture Development, Global Biological Development, Bayer HealthCare, 800 Dwight Way, Berkeley, CA 94710, USA
e-mail: chetan.goudar@bayer.com

Keywords Bioprocess development · Fed-batch culture · Logistic equations · Mammalian cell culture · Specific productivity

Introduction

Fed-batch cultivation of mammalian cells continues to be the method of choice for most commercial cell culture processes [11]. This is primarily because the majority of the licensed biopharmaceuticals are monoclonal antibodies [2, 12–14] which are relatively stable under culture conditions. Dramatic increases in antibody productivity as a consequence of cell line and process optimization have substantially driven down the cost of goods associated with cell culture [10].

Accurate quantification of cell specific rates in fed-batch cultures is a challenge with results often being influenced by the analysis approach. Logistic modeling of mammalian cell fed-batch cultures has been proposed as a robust alternative to the discrete derivative and polynomial curve fitting approaches for specific rate estimation [8] and the associated computational approach has also been described [6]. This approach results in robust time courses of specific rates related to cell growth, nutrient consumption, metabolite production, and recombinant protein production. In addition to providing valuable information on the culture and experimental conditions being studied, cell specific rates are inputs for metabolic flux analysis and accurate estimates help ensure robust metabolic flux data. This is especially important given the inherent error in experimental measurements that will propagate into the flux estimates through the specific rates [7].

An alternate application of the logistic modeling approach is for a priori analysis of a cell culture system.

Activities such as cell line development and preliminary process optimization occur early in the development cycle with limited information on cell performance. In the absence of clear targets for bioreactor protein concentration (based on material needs for toxicology and clinical trials), there can be wasteful allocation of resources towards process improvements which are perhaps best done once clinical proof of concept (PoC) has been established through human clinical trials. Moreover, the criticality of rapid advancement of a therapeutic candidate to the PoC stage has only been increasing in light of increased overall process development costs from $802 million per new drug in 2004 [4, 5] to $1,214 million in 2010 [1]. Under these circumstances, it is beneficial to identify desirable ranges for key variables such as specific protein productivity and maximum cell density in fed-batch cultures that are aligned with material needs for human clinical trials. This can help ensure optimal allocation of time and resources for each drug candidate and also facilitate the evaluation of additional candidate molecules, thereby maximizing benefit to patients.

Application of the logistic approach to describe experimental X and P data and for simulating their time courses is presented in this study. Sensitivity analysis was performed to determine the impact of each of the model parameters on X and P time courses. Subsequently, the application of this approach to simulate typical early- and late-stage mammalian cell fed-batch processes is presented.

Theory

Viable cell density

A four-parameter logistic equation has been used to describe the dynamics of mammalian cell growth and death in a fed-batch bioreactor [8]

$$X = \frac{a_1}{e^{a_2 t} + a_3 e^{-a_4 t}} \tag{1}$$

where X is the viable cell density, a_1–a_4 are model parameters, and t is time. Biological interpretations of the model parameters can be derived by exploring the limiting cases of Eq. 1. For instance, setting $a_3 e^{-a_4 t} = 0$ results in $X = a_1 e^{-a_2 t}$, an exponential decline equation such that a_2 is analogous to the maximum death (kd_{max}). Alternatively, setting $e^{a_2 t} = 0$ reduces Eq. 1 to $X = a_1 e^{a_4 t}/a_3$, an exponential growth equation, implying that a_4 is analogous to μ_{max}, the maximum growth rate. A modification of Eq. 1 to reflect the initial condition ($t = 0$) in a fed-batch experiment results in the following

$$X_0 = \frac{a_1}{1 + a_3} \tag{2}$$

where X_0 is the cell density at $t = 0$. In addition, an expression for t_{max}, the time required to reach maximum cell density in a fed-batch process, can be obtained by setting the first derivative of Eq. 1 to zero

$$t_{max} = \frac{1}{a_2 + a_4} \ln\left(\frac{a_3 a_4}{a_2}\right) \tag{3}$$

While parameters a_2 and a_4 are directly associated with classical descriptors of cell death and growth rates, such a direct interpretation of parameters a_1 and a_3 is not possible. An understanding of their impact on the cell density time course, however, is very important, and can be done using sensitivity equations, which for Eq. 1 can be derived as

$$\frac{\delta X}{\delta a_1} = \frac{X}{a_1} \tag{4}$$

$$\frac{\delta X}{\delta a_2} = -\left(\frac{X^2}{a_1}\right) t e^{a_2 t} \tag{5}$$

$$\frac{\delta X}{\delta a_3} = -\left(\frac{X^2}{a_1}\right) e^{-a_4 t} \tag{6}$$

$$\frac{\delta X}{\delta a_4} = \left(\frac{X^2}{a_1}\right) a_3 t e^{-a_4 t} \tag{7}$$

Product concentration

The accumulation of product (P) over the course of a fed-batch experiment can be described by the logistic growth equation [8]

$$P = \frac{b_1}{1 + b_2 e^{-b_3 t}} \tag{8}$$

where b_1–b_3 are the model parameters. The parameter b_1 is analogous to P_{max}, the maximum product concentration, and this can be derived by setting the derivative of Eq. 8 to zero. Parameter b_3, which is in the exponential term of Eq. 8, is analogous to a rate constant for product concentration increase. The impact of parameters b_1–b_3 on the dynamics of P can be analyzed from the sensitivity equations for Eq. 8

$$\frac{\delta P}{\delta b_1} = \frac{P}{b_1} \tag{9}$$

$$\frac{\delta P}{\delta b_2} = -\left(\frac{P^2}{b_1}\right) e^{-b_3 t} \tag{10}$$

$$\frac{\delta P}{\delta b_3} = \left(\frac{P^2}{b_1}\right) b_2 t e^{b_3 t} \tag{11}$$

Materials and methods

Analysis of experimental data

Cell density and product concentration data from two recently published antibody-producing industrial fed-batch CHO cell cultures [3, 9] were used to illustrate the applicability of the logistic equations to describe such data sets. In the first study, the lead CHO cell line expressing human IgG1 MAb 4A1 was evaluated both in 500-ml shake flasks and 2-l bioreactors. While a hydrolysate-containing feed was used in shake flask cultures, a chemically defined feed was used in the 2-l bioreactor and final product concentrations in the shake flask and bioreactor cultures were 3.0 and 4.1 g/l, respectively. Cell density and product concentration data from both the shake flask and bioreactor cultures were analyzed using the logistic equations. In the second study, CHO cells were used for antibody production in fed-batch cultures and cell density and product concentration data from two rounds of process development were analyzed using the logistic equations.

Given the nonlinear dependence of X and P on parameters a_1–a_4 and b_1–b_3 in Eqs. 1 and 8, respectively, estimation of logistic parameters was performed using nonlinear least squares. Initial estimates of parameters a_1–a_4 and b_1–b_3 were obtained using linearized versions of Eqs. 1 and 8 as described earlier [6]. These initial estimates were subsequently used to obtain the final estimates by minimizing the sum of squares error (SSE) between experimental and model fit data

$$\mathrm{SSE} = \sum_{i=1}^{n} \left[(x_{\mathrm{meas}})_i - (x_{\mathrm{fit}})_i\right]^2 \tag{12}$$

where $(x_{\mathrm{meas}})_i$ is the ith experimental cell density/product concentration value and $(x_{\mathrm{fit}})_i$ the ith model fitted value in a total of n observations.

Logistic equation sensitivity analysis

Results from logistic modeling of the shake flask data [3] were used as the basis for sensitivity analysis. Fitting Eq. 1 to the viable cell density data set resulted in a_1–a_4 estimates of 45.6×10^6 cells/ml, 0.16 day^{-1}, 62.4, and 0.48 day^{-1}, respectively, while fitting Eq. 8 to the product concentration data resulted in b_1–b_3 estimates of 3.2 g/l, 84.7, and 0.57 day^{-1}, respectively. These parameter estimates were used to generate the sensitivity curves for X and P as defined by Eqs. 4–7 and 9–11, respectively. Subsequently, for each of a_1–a_4 and b_1–b_3, two points that were 25% apart were chosen on either side of the above estimated values resulting in a total of five values (e.g., the five values for a_1 were 22.8, 34.2, 45.6, 57, and 68.4 $\times$ 10^6 cells/ml). A single parameter was varied at a time resulting in a total of five X or P profiles per parameter. An examination of these families of curves helped characterize the sensitivity of X and P to changes in a_1–a_4 and b_1–b_3, respectively.

Simulation of cell density and product concentration time courses

The utility of the logistic approach to perform a priori simulations of X and P time courses that could guide process development activities was demonstrated both for early- and late-stage fed-batch processes. The choice of the logistic parameters was in line with typical values observed in mammalian cell fed-batch cultures. A culture duration of 14 days was assumed with ranges of 0.4–0.6 day^{-1} and 0.1–0.15 day^{-1}, respectively, for maximum growth and death rates. In addition maximum cell densities ranges were 8–12 $\times$ 10^6 cells/ml in a typical early-stage process while higher values of 15–20 $\times$ 10^6 cells/ml were assumed for late-stage processes. For final product concentration, the variable of highest interest, values of 2 and 7 g/l were assumed for early- and late-stage processes, respectively. Two sets of logistic variables (a_1–a_4 and b_1–b_3) corresponding to early- and late-stage processes, respectively, and which were subject to the above constraints are shown in Table 1. Using these Table 1 values, we generated two sets of X and P time courses such that similar final product concentrations were attained but with varying cell density, cell growth, and protein productivity time courses. The objective of this exercise was to demonstrate that the multitude of paths that lead up to an early- or late-stage fed-batch process could be simulated by the logistic approach.

Results

Analysis of experimental data

Time courses of viable cell density data for CHO cells expressing human IgG1 MAb 4A1 in 500-ml shake flasks

Table 1 Logistic parameters used for simulating early- and late-stage fed-batch processes

Parameter	Early-stage process		Late-stage process	
	E1	E2	L1	L2
a_1 (10^6 cells/ml)	50.5	50.5	50.5	50.5
a_2 (day^{-1})	0.15	0.15	0.1	0.1
a_3	100	100	100	500
a_4 (day^{-1})	0.4	0.6	0.7	0.7
b_1 (g/l)	2.0	2.0	7.0	7.0
b_2	100	300	500	900
b_3 (day^{-1})	0.5	0.7	0.7	0.7

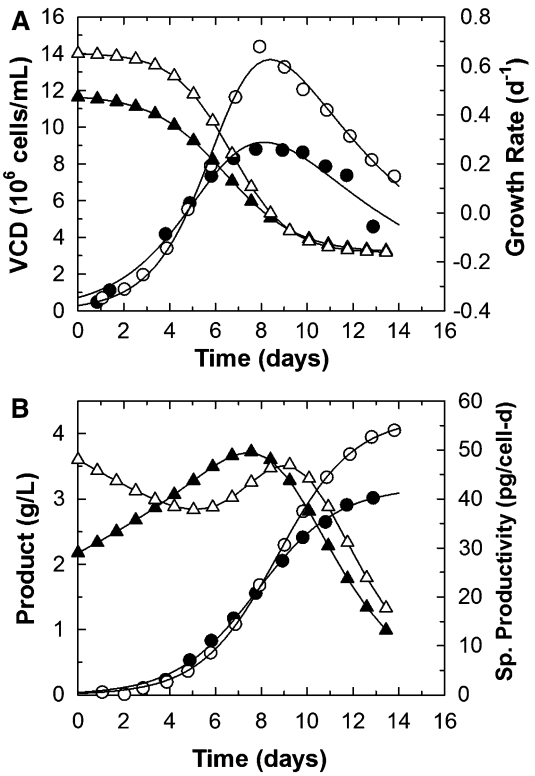

Fig. 1 Cell density, growth rate, product concentration, and specific productivity data for antibody-producing CHO cells in shake flask and bioreactor culture. The points for cell density and product concentration are experimental data [3] and the lines are fits from Eqs. 1 and 8, respectively. Growth rate and specific productivity were computed from the logistic fits as described before [8]. **a** Shake flask cell density (*filled circles*); bioreactor cell density (*open circles*); shake flask growth rate (*filled triangles*); bioreactor growth rate (*open triangles*). **b** Shake flask product concentration (*filled circles*); bioreactor product concentration (*open circles*); shake flask specific productivity (*filled triangles*); bioreactor specific productivity (*open triangles*)

Table 2 Logistic parameters and related variables for CHO cells producing human IgG1 MAb 4A1 in shake flask and bioreactor cultures

Parameter	Shake flask	Bioreactor
Viable cell density		
a_1 (10^6 cells/ml)	45.6	67.7
a_2 (d^{-1})	0.16	0.16
a_3	62.4	236.8
a_4 (d^{-1})	0.48	0.65
t_{max} (d)	8.1	8.4
X_{max} (10^6 cells/ml)	9.2	13.7
μ_{max} (d^{-1})	0.47	0.64
kd_{max} (d^{-1})	0.15	0.16
Product concentration		
b_1 (g/l)	3.2	4.3
b_2	84.7	184.6
b_3 (d^{-1})	0.57	0.60
P_{max} (g/l)	3.0	4.1
Avg. q_P (pg/cell-d)	38.2	36.5
Max. q_P (pg/cell-d)	51.4	47.6

The associated time profiles of viable cell density and product concentration (data from [3]) are shown in Fig. 1

and 2-l bioreactors are shown in Fig. 1a along with the best fit lines from Eq. 1. In both cases, the viable cell density (VCD) data were well described by Eq. 1 and cell specific growth rates calculated as described before [8] and are also shown in Fig. 1a. Time profiles of product concentration are shown in Fig. 1b along with the best fit lines from Eq. 8. Similar to VCD, the product concentration data sets were very well described by Eq. 8 resulting in smooth specific productivity profiles (Fig. 1b).

Values of the logistic parameters corresponding to the best fits in Fig. 1 are shown in Table 2 along with some additional parameters. The biggest difference in the Fig. 1a VCD profiles was the higher maximum cell density in the bioreactor. The higher growth rates in the bioreactor are best reflected in the a_4 values which were 0.65 and 0.48 day^{-1} for the bioreactor and shake flask, respectively, and were essentially the same as their maximum growth rates (0.64 and 0.47 day^{-1}, Table 2). No changes were seen in a_2 which was virtually identical to the maximum death rate (Table 2). The higher X_{max} value for the bioreactor data was an accurate representation of the experimental observations (Fig. 1a).

Very similar product concentration profiles were seen for ca. 9 days in Fig. 1b after which higher values were seen in the bioreactor. The final shake flask and bioreactor concentrations of 3.0 and 4.1 g/l, respectively, were reflected in their respective b_1 values of 3.2 and 4.3 g/l (Table 2) consistent with b_1 being an indicator of the maximum product concentration [8]. Higher b_2 values were seen for the bioreactor data (184.6 vs. 84.7) while b_3 was slightly higher (0.60 vs. 0.57 day^{-1}) in the bioreactor.

Time profiles of an antibody-producing cell line (cell line A in [9] are shown in Fig. 2a at two rounds (rounds 1 and 3) of process development. The round 3 data were characterized by higher maximum cell density (21.7 vs. 19.7 $\times$ 10^6 cells/ml) and lower values of all four Eq. 1 parameters (Table 3). Despite lower initial growth rates, the round 3 VCD data after 8 days were consistently higher than those for round 3 and this was primarily due to a lower death rate ($a_2 = 0.07$ vs. 0.11 day^{-1} for round 1 data). Unlike in Fig. 1a where higher cell densities were associated with higher growth rates, lower cell death rates (despite lower growth rates) were responsible for higher cell densities in Fig. 2a. This further highlights the multitude of paths that can result in a cell density increase and the ability of the logistic framework to identify them.

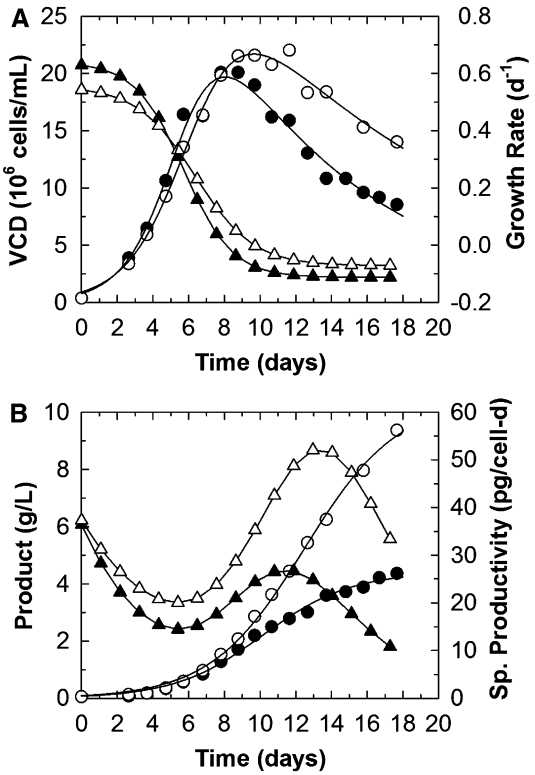

Fig. 2 Cell density, growth rate, product concentration, and specific productivity data for antibody-producing CHO cells at two rounds of process optimization. The points for cell density and product concentration are experimental data [9] and the lines are fits from Eqs. 1 and 8, respectively. Growth rate and specific productivity were computed from the logistic fits as described before [8]. **a** Round 1 cell density (*filled circles*); round 3 cell density (*open circles*); round 1 growth rate (*filled triangles*); round 3 growth rate (*open triangles*). **b** Round 1 product concentration (*filled circles*); round 3 product concentration (*open circles*); round 1 specific productivity (*filled triangles*); round 3 specific productivity (*open triangles*)

Product concentration data for the round 1 and round 3 processes are shown in Fig. 2b along with the logistic fits and resulting q_P values. The b_1 values were 4.4 and 10.4 g/l, respectively, consistent with maximum product concentrations of 4.2 and 9.8 g/l. The values for b_3 were similar for both data sets (0.41 and 0.38 day^{-1}) while b_2 was higher for the round 3 process, similar to that in Fig. 1b. Overall, the data in Figs. 1 and 2 suggest that logistic parameters (especially a_2 and a_4 in Eq. 1 and b_1 and b_3 in Eq. 8) for industrial fed-batch processes provide valuable insights into the kinetics of cell density and product concentration time courses and can help rationally direct process development activities.

Sensitivity analysis

The shake flask data set (Fig. 1) for CHO cells expressing human IgG1 MAb 4A1 served as the basis for sensitivity analysis. The sensitivity curves as defined by Eqs. 4–7 and 9–11 are described first followed by results from varying a_1–a_4 and b_1–b_3 around the Table 2 values which resulted in five time courses of X or P for each parameter.

Table 3 Logistic parameters and related variables for antibody-producing CHO cells during two rounds of process optimization

Parameter	Round 1	Round 3
Viable cell density		
a_1 (10^6 cells/ml)	57.2	48.9
a_2 (d^{-1})	0.11	0.07
a_3	73.7	53.6
a_4 (d^{-1})	0.64	0.55
t_{max} (d)	8.0	9.6
X_{max} (10^6 cells/ml)	19.7	21.7
μ_{max} (d^{-1})	0.63	0.54
kd_{max} (d^{-1})	0.11	0.07
Product concentration		
b_1 (g/l)	4.4	10.4
b_2	62.3	117.7
b_3 (d^{-1})	0.41	0.38
P_{max} (g/l)	4.20	9.8
Avg. q_P (pg/cell-d)	19.1	33.3
Max. q_P (pg/cell-d)	27.4	54.4

The associated time profiles of viable cell density and product concentration (data from [9]) are shown in Fig. 2

Viable cell density

The a_1–a_4 values for the shake flask data from Table 2 were used and the resulting sensitivity curves as defined by Eqs. 4–7 are shown in Fig. 3 along with the X time course. The sensitivity of a_1 follows the X time course (Fig. 3a) consistent with Eq. 4. Parameter a_2 does not impact X in the initial phase (the first 4 h in Fig. 3b) but subsequently has an inverse relationship. The parameter a_3 sensitivity curve has a decreasing followed by an increasing trend and levels off close to zero after ca. 10 days (Fig. 3c). The sensitivity curve for parameter a_4 has an increasing followed by a decreasing trend with values approaching zero towards the end of the culture (Fig. 3d).

Results from varying a_1–a_4 around the Fig. 3 values are shown in Fig. 4. Increasing a_1 resulted in an increase in X values over the entire time course (Fig. 4a), consistent with the Fig. 3a observation where the sensitivity curve for a_1 followed the entire X time course. The largest impact of a_2 was in the 6- to 14-day period where higher a_2 values reduced the maximum cell density that was attained by the culture (Fig. 4b). This is consistent with the Fig. 3b sensitivity curve and is also expected because a_2 is the maximum cell death rate. Parameter a_3 had an inverse impact on the cell density curve in the 0- to 10-day phase (Fig. 4c), consistent with the prediction from Fig. 3c. From Fig. 4d,

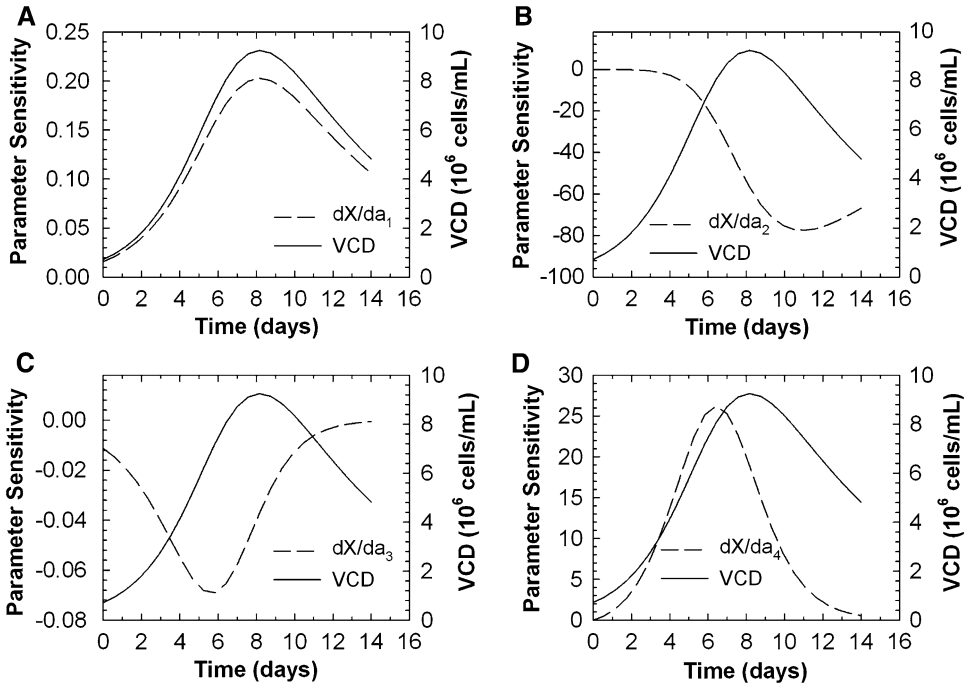

Fig. 3 Sensitivity curves for the Eq. 1 parameters a_1–a_4 (at $a_1 = 45.6 \times 10^6$ cells/ml, $a_2 = 0.16$ day^{-1}, $a_3 = 62.4$, and $a_4 = 0.48$ day^{-1}) computed from Eqs. 4–7, respectively, along with the corresponding X time course

the impact of parameter a_4 was seen over a large part of the cell density curve and the cell density profiles converged towards the very end of the culture, consistent with predictions from Fig. 3d.

Two additional parameters, the maximum cell density (X_{max}) and the time required to reach the maximum cell density (t_{max}), are also of interest in a fed-batch culture. While t_{max} can be determined from Eq. 3, X_{max} can be determined by substituting $t = t_{max}$ in Eq. 1. The impact of changes in parameters a_1–a_4 on X_{max} is shown in Fig. 5. Increase in a_1 had a proportional increase in X_{max} (Fig. 5a) while an increase in a_2, the death rate, decreased X_{max} as expected (Fig. 5b). Parameter a_3 was inversely related to X_{max} but the dependence was not as pronounced as with the other parameters (Fig. 5c). Parameter a_4, the growth rate, was positively correlated with X_{max} and also had a high impact on X_{max} (Fig. 5d).

Figure 6 shows t_{max} values as a function of changes in parameters a_1–a_4. Parameter a_1 had no impact on t_{max} (Fig. 6a) while a decreasing trend was seen for an increase in parameter a_2 (Fig. 6b), consistent with a_2 being the maximum death rate. A slight t_{max} increase was seen with increasing a_3 (Fig. 6c) while a substantial t_{max} decrease was seen with increase in a_4, the maximum growth rate (Fig. 6d).

Product concentration

The sensitivity curves for product concentration were computed from Eqs. 9–11 and are shown in Fig. 7 along with the product concentration time course. Similar to the impact of a_1 on X in Fig. 3a, the sensitivity curve for parameter b_1 followed the time course of P (Fig. 7a), consistent with Eq. 9 and can thus be expected to impact the entire P versus t curve. Parameter b_2 was negatively correlated with P and the sensitivity curve was characterized by a decreasing followed by an increasing trend that approached zero towards the end of the culture (Fig. 7b). Parameter b_3 was positively correlated with P and was characterized by an increasing followed by a decreasing sensitivity curve (Fig. 7c).

Actual product concentration time profiles for varying values of b_1–b_3 (two points on either side of the Table 2 values for shake flask culture, each 25% apart) are shown in Fig. 8. Variable b_1 has a substantial impact on the entire time course of P, consistent with Fig. 7a, and is also representative of the maximum product concentration. Variable b_2 negatively impacts the product concentration profiles and the highest impact is seen between 2 and 12 h (Fig. 8b), consistent with the Fig. 7b sensitivity curve. Variable b_3 has a positive impact on P which is pronounced after 2 h (Fig. 8c) in line with the observations in Fig. 7c.

Simulation of X and P in fed-batch cultures

Early-stage development projects are typically associated with non-optimal cell lines, medium formulations, and culture conditions and usually have maximum cell densities in the 8–12 $\times$ 10^6 cells/ml range. Suboptimal culture conditions can result in lower cell growth rate and/or higher cell death rates due to nutrient limitations. X and P time courses along with those for growth rate and specific productivity for two representative early-stage

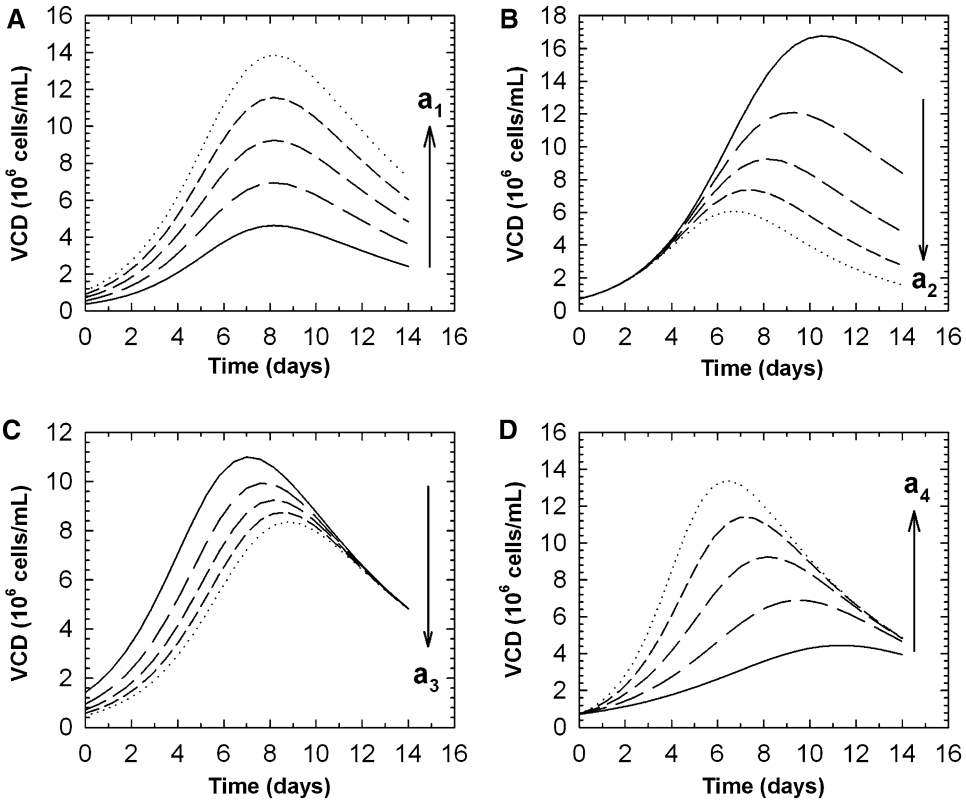

Fig. 4 Sensitivity of X to changes in a_1–a_4. Baseline parameter values are from Fig. 3 with two values on either side, each 25% apart. The *arrow* indicates the direction of parameter value increase

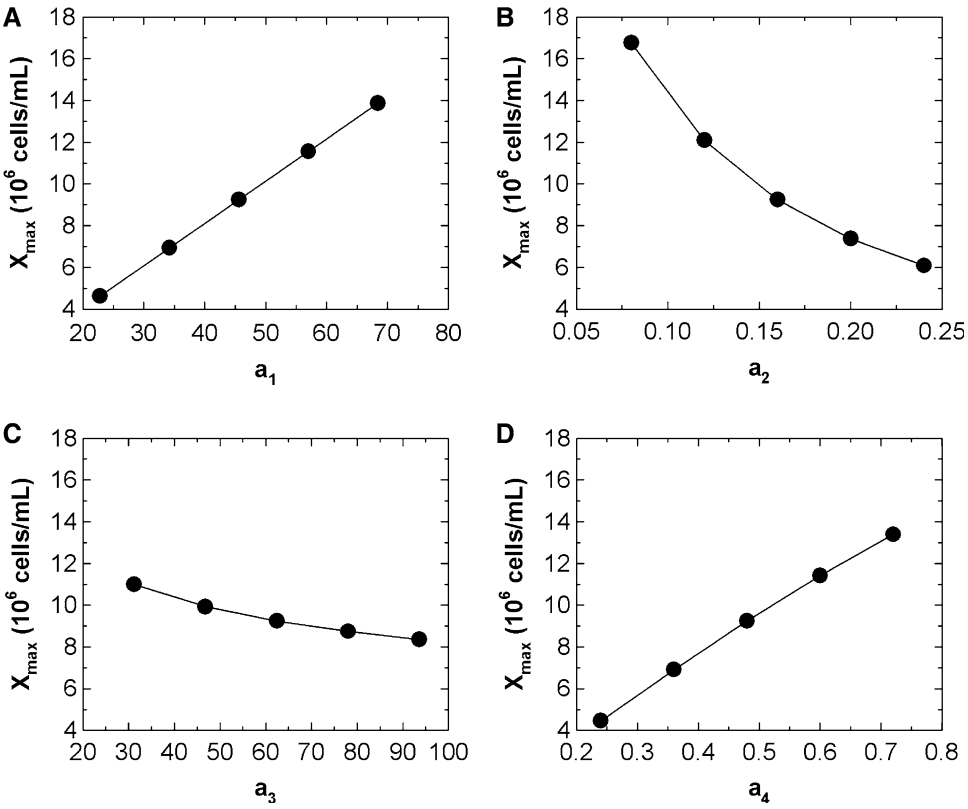

Fig. 5 Changes in X_{max} as a function of changes in parameters a_1–a_4. X_{max} was most sensitive to changes in a_1 followed by those in a_2 and a_4. Parameter a_3 had the least impact on X_{max}

processes E1 and E2 were generated using Table 1 a_1–a_4 and b_1–b_3 values and are shown in Fig. 9a, b. While both processes resulted in a final product concentration of 2 g/l (Fig. 9b), there were differences in the cell density, growth, product concentration, and productivity profiles. For instance, increasing a_4 from 0.4 to 0.6 day^{-1} in Eq. 1

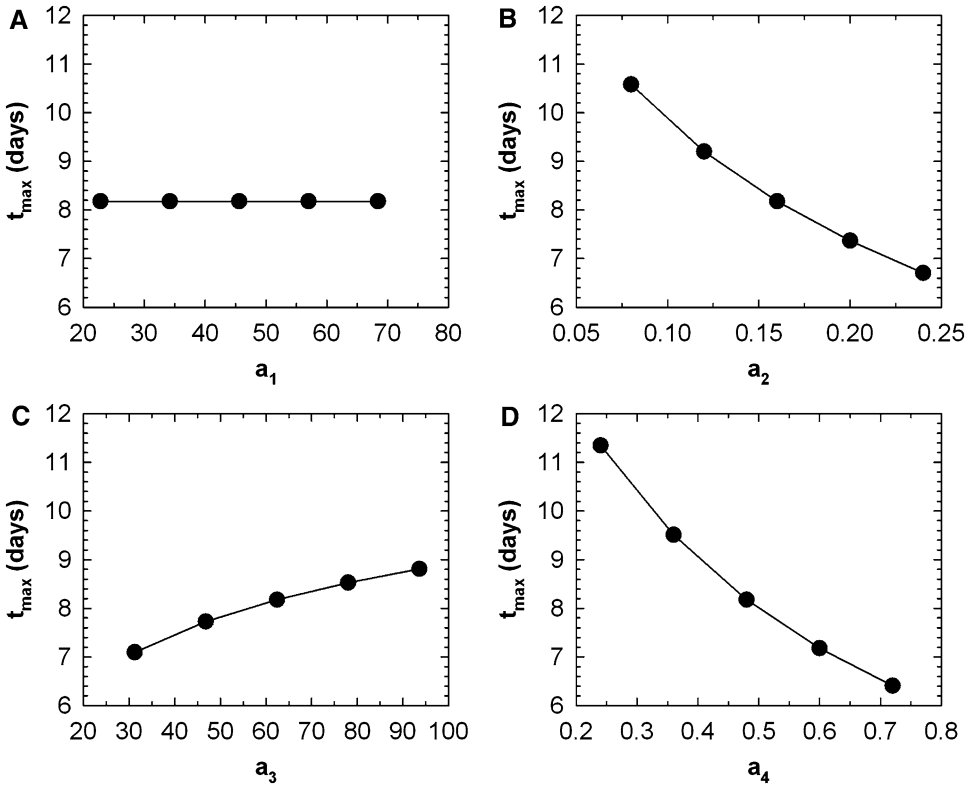

Fig. 6 Changes in t_{max} as a function of changes in parameters a_1–a_4. t_{max} was most sensitive to changes in a_4, followed by those in a_2 and a_3 and was independent of a_1

resulted in an X_{max} increase from 8 to 12.1 × 10^6 cells/ml and was also associated with a t_{max} reduction from 10.2 to 8 days (Fig. 9a), consistent with the information in Figs. 3–6. Because of this cell number increase, lower average specific productivities (16.3 vs. 26.3 pg cell^{-1} day^{-1}) were adequate for the high cell density case to reach the final product concentration of 2 g/l (Fig. 9b). Increases in b_2 (100–300) and b_3 (0.5–0.7 day^{-1}) counteracted each other as suggested by the Fig. 7 sensitivity curves such that the overall impact on the product concentration profile was small (Fig. 9b). The corresponding q_P profiles, however, were much different and this was largely due to the difference in the Fig. 9a VCD profiles.

Data representative of a more mature fed-batch process with final product concentrations of 7 g/l are shown in Fig. 9c, d for late-stage processes L1 and L2 using a_1–a_4 and b_1–b_3 values from Table 1. A fivefold increase in a_3 from 100 to 500 resulted in an X_{max} decrease from 19.5 to 15.9 × 10^6 cells/ml and an increase in t_{max} from 8.2 to 10.2 days (Fig. 9c), consistent with the sensitivity predictions in Fig. 3–6. Because a_2 and a_4 were unchanged, the terminal and initial growth rate values were similar for both data sets in Fig. 9c and were very close to their respective a_2 and a_4 values of 0.1 and 0.7 day^{-1}. An increase in b_2 from 500 to 900 had a minimal impact on the product concentration profile in Fig. 9d, consistent with the sensitivity curves in Fig. 8b. Like in Fig. 9b, the specific productivity profiles in Fig. 9d were different with the higher cell density data associated with lower average q_P values (33.6 vs. 56.3 pg cell^{-1} day^{-1}).

Overall, the Fig. 9 data reinforce common knowledge that multiple process development approaches that manifest as varying cell density, growth, and protein production time profiles can result in the desired final product concentration. The logistic framework presented in this study allows a priori visualization of these multiple paths and can help direct process development activities such that the desired product concentrations are reached with minimal time and resource use.

Discussion

The logistic equations provide a means for modeling cell density and product concentration time courses in mammalian cell fed-batch reactors. Despite the non-mechanistic nature of the logistic equations, time profiles are logically constrained (cell density time courses are characterized by increasing followed by decreasing trends; product concentration time courses are characterized by increasing values with an asymptotic maximum) which makes them an ideal candidate for simulating cell density and product concentration trends. Such simulations are helpful in the development of both early- and late-stage fed-batch processes where product requirements are substantially

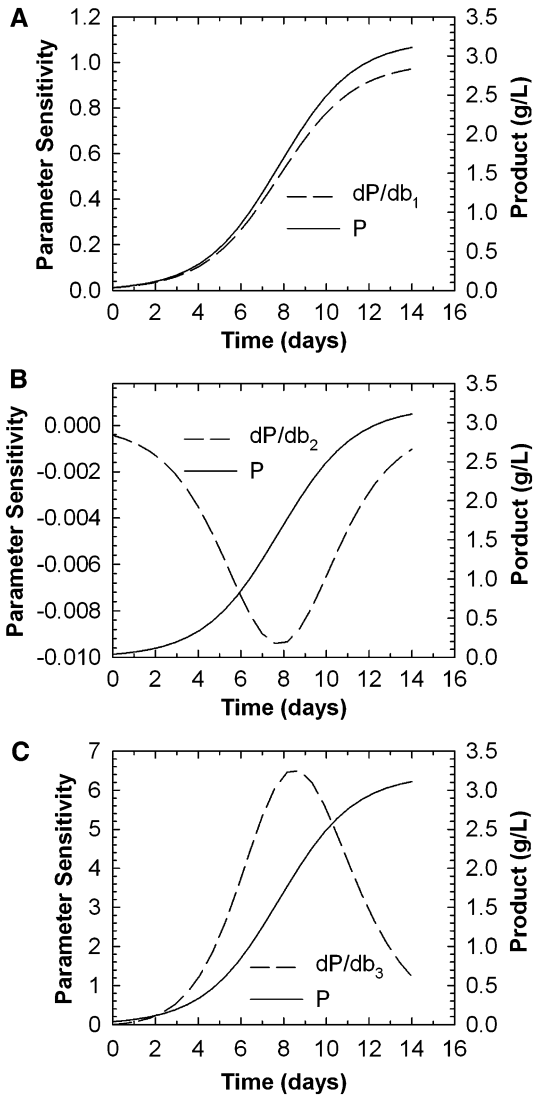

Fig. 7 Sensitivity curves for the Eq. 8 parameters b_1–b_3 (at $b_1 = 3.2$ g/l, $b_2 = 84.7$, and $b_3 = 0.57$ day^{-1}) computed from Eqs. 9–11, respectively, along with the corresponding P time course

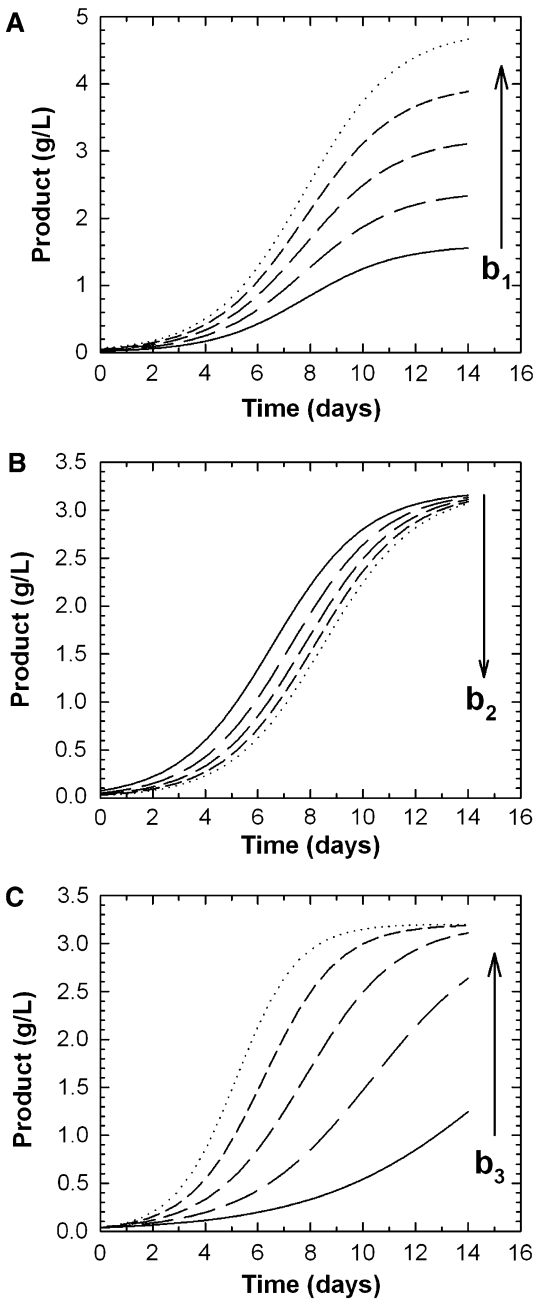

Fig. 8 Time courses of product concentration for changes in parameters b_1–b_3. Baseline parameter values are from Fig. 7 with two other values on either side, each 25% apart. The *arrow* indicates the direction of parameter value increase

different. The conventional approach for determining process development benchmarks is primarily focused on product concentration, which, albeit pragmatic and simple, does not taken into account the multitude of paths that can lead to that target. Simulations using the logistic equations can help determine a priori estimates for cell growth and death rates and specific productivity, or combinations thereof, which can result in the desired final product concentration. For instance, if a target final product concentration of 1–2 g/l is desired, selection of a clone with an average q_P of 10–20 pg cell^{-1} day^{-1} should be adequate if cell densities on the order of 10×10^6 cells/ml can be reached during the course of the cultivation. This insight can help streamline cell line development by rational allocation of resources because time-consuming steps such as amplification or screening of additional clones in the pursuit of a higher producer can be avoided. Alternatively, if much higher product concentrations are desired and cell line changes cannot be made, these simulations can help medium and process optimization efforts by providing targets for growth and death rates and protein productivity.

Despite the intuitiveness of the simulations presented in this study, there are limitations. Not all parameter combinations will result in time courses of X, P, μ, and q_P that are

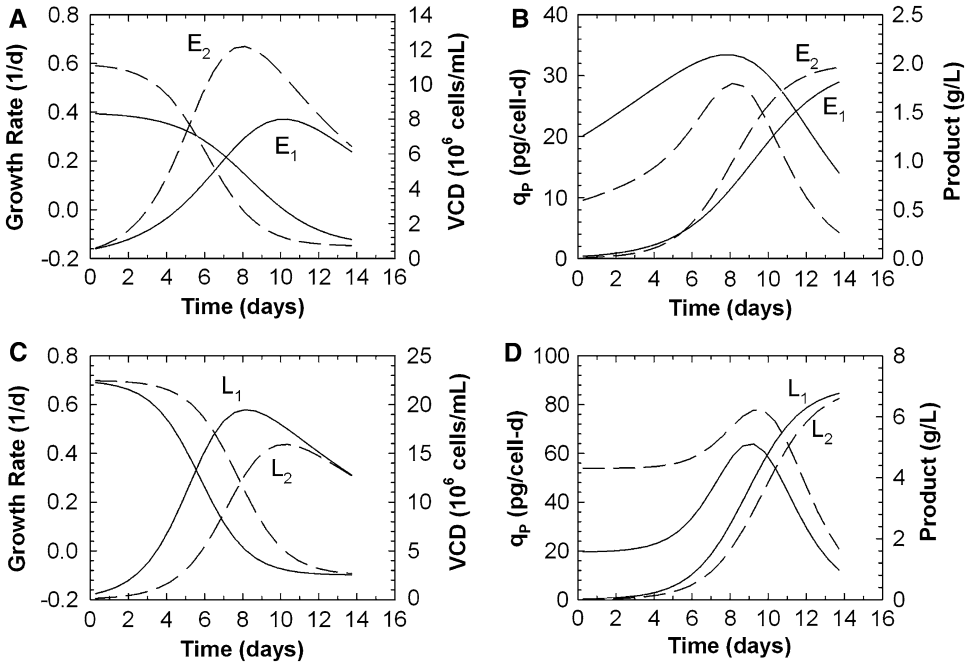

Fig. 9 Logistic equation simulations for cell density and product concentration time courses for two representative early-stage (E_1 and E_2 in **a**, **b**) and late-stage (L_1 and L_2 in **c**, **d**) fed-batch processes. The logistic parameters used for these simulations are shown in Table 1

biologically representative. It is thus important to understand the sensitivity of X and P to parameters a_1–a_4 *and* b_1–b_3 as described in Figs. 3–8 which can guide the user towards rational use of the logistic models for X and P simulation. Furthermore, time courses resulting from any simulation exercise must be carefully evaluated to ensure consistency with published work on mammalian cell fed-batch cultures and previous experience with the cell line of interest. Every attempt must be made to arrive at first principles based interpretation of the time courses. When used judiciously, the logistic equation based simulation approach presented in this study can be a useful tool for supporting fed-batch cell culture process development.

Conclusions

In summary, logistic equations were used to simulate time courses of viable cell density, growth rate, product concentration, and cell specific protein production for mammalian cells in fed-batch culture. The resulting time profiles were logically constrained by the logistic equations and scenarios reflective of early- and late-stage cell culture processes could be readily simulated by an appropriate choice of model parameters. Such simulations can guide process development activities by helping define rational targets for cell growth and protein productivity. By providing additional insights into the dynamics of cell growth and protein production over the entire duration of the culture, the simulations are an improvement over the current paradigm where only final product concentration in the bioreactor drives process development activities. Through thoughtful selection of model parameters and a careful analysis of the resulting time course, it is possible to have some general kinetic understanding of the system being studied. The ease with which this can be done using the logistic equations should help accelerate both early- and late-stage fed-batch cell culture process development activities.

Acknowledgments Insightful perspectives on the implications of final product concentration on process development and commercial manufacturing from Paul Wu, Harald Dinter, and Clive Wood, all of Bayer HealthCare, are appreciated.

References

1. Adams CP, Brantner VV (2010) Spending on new drug development. Health Econ 19:130–141
2. Aggarwal S (2007) What's fueling the biotech engine? Nat Biotechnol 25:1097–1104
3. Combs RG, Yu E, Roe S, Piatchek MB, Jones HL, Mott J, Kennard ML, Goosney DL, Monteith D (2011) Fed-batch bioreactor performance and cell line stability evaluation of the artificial chromosome expression technology expressing an IgG1 in Chinese hamster ovary cells. Biotechnol Prog 27:201–208
4. DiMasi R, Hansen HA, Grabwoski H (2003) The price of innovation: new estimates of drug development costs. J Health Econ 22:151–185
5. DiMasi R, Hansen R, Grabwoski H (2004) R&D costs and returns by therapeutic category. Drug Inf J 38:211–223
6. Goudar CT (2009) Robust parameter estimation during logistic modeling of batch and fed-batch culture kinetics. Biotechnol Prog 25:801–806
7. Goudar CT, Biener R, Konstantinov KB, Piret JM (2009) Error propagation from prime variables into specific rates and metabolic fluxes for mammalian cells in perfusion culture. Biotechnol Prog 25:986–998

8. Goudar CT, Joeris K, Konstantinov K, Piret JM (2005) Logistic equations effectively model mammalian cell batch and fed-batch kinetics by logically constraining the fit. Biotechnol Prog 21:1109–1118
9. Huang Y-M, Hu W, Rustandi E, Chang K, Yusuf-Makagiansar H, Ryll T (2010) Maximizing productivity of CHO cell-based fed-batch culture using chemically defined media conditions and typical manufacturing equipment. Biotechnol Prog 26:1400–1410
10. Kelley BD (2007) Very large scale monoclonal antibody purification: the case for conventional unit operations. Biotechnol Prog 23:995–1008
11. Kelley BD (2009) Industrialization of mAB production technology. The bioprocessing industry at a crossroads. mAbs 1:441–452
12. Kozlowski S, Swann P (2006) Current and future issues in the manufacturing and development of monoclonal antibodies. Adv Drug Deliv Rev 58:707–722
13. Krishnan M (2007) Monoclonal antibody gold rush. Curr Med Chem 14:1978–1987
14. Reichert JM (2009) Global antibody trends. mAbs 1:86–87